Catalysis Today 369 (2021) 227–234

Contents lists available at ScienceDirect

Catalysis Today

journal homepage: www.elsevier.com/locate/cattod

Understanding of K and Mg co-promoter effect in ethylene oxychlorination by operando UV–vis-NIR spectroscopy

Hongfei Ma [a], Endre Fenes [a], Yanying Qi [a], Yalan Wang [a], Kumar R. Rout [a,b,*], Terje Fuglerud [c], De Chen [a,*]

[a] Department of Chemical Engineering, Norwegian University of Science and Technology, Sem sælands vei 4, N-7491, Trondheim, Norway
[b] Sintef Industry, Sem sælands vei 2A, N-7491, Trondheim, Norway
[c] INOVYN, Herøya Industrial Park, N-3936, Porsgrunn, Norway

ARTICLE INFO

Keywords:
Ethylene oxychlorination
$CuCl_2/\gamma$-Al_2O_3-based catalyst
Co-promoter effect
Operando study
Rate-diagram

ABSTRACT

The comprehensive kinetic study for $CuCl_2/\gamma$-Al_2O_3-based catalysts was performed to elucidate the co-promoter effect in the ethylene oxychlorination, one of the most significant industrial processes to produce vinyl chloride monomer. Kinetic analysis was performed separately by transient kinetic studies, taking account of the reduction and oxidation steps in the catalytic cycle. The promoter effects on ethylene oxychlorination were ascribed to their influence on the Cu^{2+} reduction or Cu^{+} oxidation in the catalytic cycle. The reaction rate-diagram was gained and used to predict the steady-state reaction rate and Cu oxidation state by an operando setup combing MS and UV–vis-NIR spectroscopy. The results indicated that the K-doped catalyst could greatly increase the reaction rate of the oxidation step, which gave rise to higher Cu^{2+} concentration on the catalyst. Mg-doped catalyst had a great effect on enhancing the reaction rate for the reduction step. K and Mg co-doped catalyst had the dual effect, both the reaction rate and Cu oxidation state were located between K and Mg mono-doped catalyst. The results of steady-state reactions indicated that the reaction rates were quite close with that predicated by the rate-diagram. Byproduct analysis during the steady-state was also performed, the results demonstrated that the co-promoted catalysts can also reduce the byproduct formation. The current study is expected to provide one way for exploring the potential benefits of co-promotion on $CuCl_2/\gamma$-Al_2O_3-based industrial oxychlorination catalysts to improve the catalytic performance and understand the reaction further.

1. Introduction

Polyvinyl chloride (PVC) is one of the most commonly used plastics in the world. It is produced through the polymerization of its monomer vinyl chloride (commonly called VCM in abbreviation) [1–3]. Because of the increasing demand for PVC in the world, which is making VCM one of the most important chemicals in the industry. There are several different ways to produce VCM in the industry, based on the resource materials used, mainly from ethane, ethylene, and acetylene [4–9]. Ethylene oxychlorination is one of the most important and commonly used ways in European countries. Many efforts have been devoted to the study of the ethylene oxychlorination process [10–15]. It is commonly called as a balanced VCM process in the industry. In brief, ethylene dichloride (EDC) was firstly produced through ethylene oxychlorination or direct ethylene chlorination, followed by thermal cracking of EDC to form VCM, with HCl recycled simultaneously, which is highly efficient and environmentally friendly. $CuCl_2/\gamma$-Al_2O_3 is commonly used as the active catalyst in the industry, while copper loss and particle agglomeration causing the deactivation of the catalyst are still the main challenges for the commercial catalysts in the industry, which is related to the Cu^{+} concentration of the catalyst [3,9,11,16]. So, promoters such as alkali and alkali earth metals like K, Na, and Mg are used as the promoters to improve the catalytic performance like preventing the copper loss and agglomeration [11,12,16–19]. Many studies have been reported about ethylene oxychlorination on the reaction mechanism studies. The oxychlorination process follows the overall reaction as Eq. 1 [11,16,18,20–23].

$$C_2H_4 + 0.5O_2 + 2HCl \rightarrow C_2H_4Cl_2 + H_2O \quad (1)$$

* Corresponding authors at: Department of chemical engineering, Norwegian University of Science and Technology, Sem sælands vei 4, N-7491, Trondheim, Norway.
E-mail addresses: kumarranjan.rout@sintef.no (K.R. Rout), de.chen@ntnu.no (D. Chen).

https://doi.org/10.1016/j.cattod.2020.06.049
Received 14 October 2019; Received in revised form 15 May 2020; Accepted 13 June 2020
Available online 23 June 2020

It is commonly accepted that the total reaction can be divided into three steps, following Eqs. 2–4:

Reduction of $CuCl_2$ to CuCl by C_2H_4

$$2CuCl_2 + C_2H_4 \rightarrow C_2H_4Cl_2 + 2CuCl \quad (2)$$

Oxidation of CuCl to copper oxychloride by O_2

$$2CuCl + 0.5O_2 \rightarrow Cu_2OCl_2 \quad (3)$$

Hydrochlorination of copper oxychloride to $CuCl_2$ by HCl

$$Cu_2OCl_2 + 2HCl \rightarrow 2CuCl_2 + H_2O \quad (4)$$

While the mechanism was still not fully understood even though the long period of fundamental and industrial researches on it. However, from the proceeding related researches, the oxidation process is the rate determine step for the neat Cu catalyst [16]. What is more, because of the volatile properties of Cu^+ [20,24–26], more attention was paid to the oxidation step, to enhance the oxidation rate of CuCl. As mentioned above, promoters like K, Mg, and Na are used to decrease the loss of Cu^+, which would affect the performance of the catalyst, like reduction rate or oxidation rate. Lamberti and co-authors systematically studied the properties of the Al_2O_3 supported $CuCl_2$ catalyst [20,24–28]. It is commonly accepted that part of $CuCl_2$ is monolayer dispersed on the surface of Al_2O_3, the rest of Cu is bonded with Al_2O_3 [29–32]. While the former is served as the active site, the latter is non-active for the reaction. Adding K and Mg can increase the amount of reducible $CuCl_2$ on the catalyst. Furthermore, researches have been devoted to the effects of promoters in product selectivity and activity [33]. They have demonstrated that promoters like K and La, could give rise to superior ethylene activity and lower byproduct formation by increasing the active Cu species while at the same time covering the Lewis and Brønsted acid sites on the supports [33]. They have demonstrated that adding KCl is able to displace the rate-determining step from the CuCl oxidation to the $CuCl_2$ reduction step, while not for Mg.

UV–vis-NIR spectroscopy is widely used in the research on transition metal ions in heterogeneous catalysis. Two bands can be observed on the spectroscopy, one measures d-d transitions, the other one for charge transfer. The d-d transition bands yield information on the oxidation state and the coordination environment [34]. The d-d transition bands yield information on the oxidation state and the coordination environment. As Cu^+ does not exhibit a d-d band in the d-d transition region, the decreasing amount of Cu^+ and increasing amount of Cu^{2+} resulted in the increasing Kubelka-Munk function (KMF). Thus, the change in KMF units can be used to reflect the oxidation state changing of Cu between Cu^+ and Cu^{2+}. A linear relationship between the catalyst total Cu^{2+} concentration and the normalized KMF (NKMF) units for the reduction and oxidation steps was obtained, it can be used to quantify the Cu^{2+} concentration [22]. In our previous report, we combined the UV–vis-NIR and mass spectra (MS) as the operando technique to study the reaction mechanism and kinetics [16,22,23], which was proved to be a relatively simple *in situ* method compared to XANES and EXAFS. By using this technique, we can monitor the process of Cu^{2+} to Cu^+ transformation, and Cu^{2+} regeneration. A rate-diagram was proposed to predict and analyze the reaction rate with Cu profiles during steady-state experiments. We investigated the roles of promoters, such as Ce, K, La in the process of oxychlorination. Especially the influence on the reaction rates of the reduction and oxidation steps in the redox cycle. We found that both transient and steady-state reactions were influenced by Cu^{2+} concentration, the key factor for high activity, selectivity, and stability for ethylene oxychlorination.

In the present work, K and (or) Mg dopants are added to the catalysts as the promoter (s), which are the most important promoter of industrial oxychlorination catalysts. The kinetic study is used to elucidate the co-promote effect both in transient and steady-state experiments by using our home-made operando setups combined MS and UV–vis-NIR spectroscopy. Both the transient and steady-state experiments are performed to gain a better understanding of the promoter effect on ethylene oxychlorination. The reaction rate-diagram obtained from the reduction and oxidation steps illustrates that both K and Mg promoters can increase the reducible Cu^{2+} on the catalysts. While K can significantly increase the reaction rate of oxidation than reduction; Mg enhances the reduction reaction rate more than the oxidation step. The co-doping of K and Mg compromises the effect of K and Mg mono-promoted. The steady-state experiment results show that the reaction rates are quite close to those predicted by the reaction rate-diagram.

2. Experimental methods

2.1. Catalysts preparation

All catalysts were prepared by the incipient wetness impregnation method, which was commonly reported on this type of catalyst [22–27]. The precursors ($CuCl_2$, KCl, and $MgCl_2$) were co-impregnated on Al_2O_3, and then the samples were dried at room temperature for 10 h. After that, the catalysts were put into the oven at 120 °C for 6 h with a ramping rate of 2 °C /min. All the catalysts contain 5 wt% Cu, the promoters were added with designed molar ratios to Cu, e.g. 0.4K5Cu contains 5 wt% Cu and a K: Cu molar ratio of 0.4.

2.2. Experiment set up and steps

Simplified operando setups with an efficiently fixed bed reactor were reported in our previous research. Experiments were performed in a fixed bed reactor with a dimension of 16*10*5 mm with an optical grade window, which is used for the collection of high quality of UV–vis-NIR (Avantes, Netherlands) data. The composition of reactant and products were analyzed online by an online MS (Omnistar GSD 3010: Pfeiffer Vacuum, Germany).

2.2.1. Transient-State experiments

Both transient and steady-state experiments were performed at 230 °C and a total pressure of 1 bar, with a total gas flow rate of 180 ml/min. Reactant gases were introduced into the reactor step-by-step with different mass flow controllers. Before reaction, the catalyst was heated to 230 °C in Ar with the ramping rate of 10 °C/min. During the reaction, Ar was used as diluted gas, and He as a tracer. Before redox experiments, the catalyst was activated by HCl for 4 min. The desired partial pressures for reduction and oxidation are 0.1 bar. In the reduction process, diluted ethylene was introduced to the reactor for 20 min. At the same time, the products were analyzed by an online-MS for calculating the conversion and reaction rates, and Cu^{2+} concentration monitored by UV–vis-NIR. After reduction, the reactor was flowed with Ar for at least 15 min to purge out the left reactant gas. Then, the oxidation was proceeded for 20 min by introducing the diluted O_2. The reactor was again purged by Ar for 15 min. Followed by the closure of the catalytic cycle with HCl for 4 min to restore the original $CuCl_2$. The second and third cycles were performed with the same procedures as above.

2.2.2. Steady-State experiments

During the steady-state reaction, all the reactants ethylene, oxygen, and hydrogen chloride diluted in Ar were introduced into the reactor with He as the tracer. The effluent gases were analyzed by an online-MS. The UV–vis-NIR data was recorded by keeping the probe at the top of the catalyst bed. The steady-state experiments were performed with the stoichiometric ratio, with the total flow rate of 180 ml/min, the partial pressures of $P_{C_2H_4}$ =0.08 bar. The reactant gasses flow was switched to GC during the steady-state twice for byproduct analysis.

2.3. Catalysts characterization

XRD profiles were recorded with a Bruker D8 Davinci X-ray diffractometer, using Cu Ka1 (0.154 nm) wavelength. The BET surface

area, BJH pore size, and pore volume were determined by nitrogen sorption at 77 K on a Micromeritics TriStar 3000 instrument.

2.4. Ethylene temperature programmed reduction

Ethylene temperature-programmed reaction (C_2H_4-TPR) was performed in the fixed bed reactor, with an online MS recording the signal. Before the TPR test, the catalysts were treated with the same two cycles with transient state experiments as described above. After the catalysts were fully oxidized to Cu^{2+}, the catalyst was then reduced by 30 % C_2H_4 with a flow rate of 120 ml/min. The product of EDC was recorded by an online MS, while the temperature was increased to 230 °C at a ramp rate of 2 °C/min.

3. Results and discussion

3.1. Catalysts properties

Fig. 1 shows the XRD patterns for the catalysts with or without a promoter. From the figure, we can see that $CuCl_2$ is still undetectable by XRD because of the high dispersion of all the catalysts, which was reported in the previous research on that $CuCl_2$ was monolayer dispersed on the Al_2O_3 surface [19,22,23,29]. Also, as shown in Fig. 1b, no Cu can be observed on the TEM image for the neat Cu catalyst. It is also reported that adding promoters, like K, Mg can increase the $CuCl_2$ dispersion on the alumina surface [7]. Therefore, $CuCl_2$ is also well dispersed on the promoted catalysts. There are almost no obvious changes in the peaks for the catalysts when the catalyst is doped with K and (or) Mg since only Al_2O_3 peaks are observed. The texture properties like BET surface area, pore volume, and pore size are listed in Table 1. The results show that the texture properties are not significantly changed by doping of promoters. Together with XRD results, it can be assumed that there are no structural differences among the catalysts with adding promoters.

3.2. Transient kinetic experiments

3.2.1. Kinetic analysis of $CuCl_2$ reduction

EDC is produced by ethylene reacting with $CuCl_2$ in the reduction step, while Cl is attracted from $CuCl_2$ on the catalyst [16,22,23]. Therefore, Cl vacancies are created as the reaction proceeding, the catalyst is reduced from $CuCl_2$ to CuCl. The amount of active Cu^{2+} participated in the reaction can be calculated from the number of C_2H_4 consumed in the reaction from mass balance. Theoretically, all the Cu^{2+} on the catalyst can be reduced to Cu^{+}, hence the fraction of reducible Cu^{2+} and Cl available on the catalyst is 1 mol/mol_{Cu}. However, as reported by the literature, not all the Cu^{2+} can be reduced to Cu^{+}, due to the interaction of Cu with the support forming an inert Cu phase, and this part of Cu^{2+} cannot be reduced to Cu^{+}. The evolution of Cu^{2+} concentration with time on stream for the (un)doped catalyst is shown in Fig. 2a. Herein, the total Cu^{2+} in the figure is the sum of the reducible Cu^{2+} with activity, and inactive Cu^{2+} fraction retains in the support per mol of atomic Cu. From the results, we can see that the amount of active Cu^{2+} increased by adding the promoters. For the neat 5Cu catalyst the removable Cu^{2+}, which is also called active Cu^{2+} is only 0.61 mol/-mol_{Cu}. When the catalyst is doped with Mg, the reducible Cu^{2+} was significantly increased to 0.79 mol/mol_{Cu} compared to the neat 5Cu catalyst. The initial turn over frequency (TOF, based on the start conversion and the Cu loading) of the reduction step is displayed in Fig. 2b. From the results, we can firstly see that the doped catalysts not only increase the reducible Cu^{2+} but also the TOF compared to the neat 5Cu catalyst. While the Mg-doped catalyst increased the most than the other two doped catalysts. The initial reduction rate for 0.4K5Cu was only greatly decreased compared to the neat 5Cu catalyst, which we have systematically studied the effect in the previous report [23].

Table 1
Physical properties and the promoter molar ratio to Cu in the catalysts

Catalyst	Surface area (m^2/g)	Pore volume (cm^3/g)	Pore size (Å)	K/Cu molar ratio	Mg/Cu molar ratio
5Cu	137	0.39	91	–	–
0.4K5Cu	128	0.37	91	0.4	–
0.4Mg5Cu	133	0.37	89	-	0.4
0.3K0.1Mg5Cu	141	0.40	88	0.3	0.1

To have a deeper understanding of the promoter effect on the reduction step. Ethylene temperature-programmed reduction was performed. Before running the C_2H_4-TPR, one catalytic redox cycle was done firstly to make the catalyst was fully oxidized to Cu^{2+}. The TPR profiles for all the catalysts are shown in Fig. 3. Herein, the temperature was only increased to 230 °C, so the Cu^{2+} can only be reduced to Cu^{+}, no Cu was formed according to the literature, reported that the temperature needed to furtherly to reduce CuCl to Cu is above 400 °C [35,36]. We should also mention that, based on the discussion above, the Cu was monolayer dispersed on all the catalysts. Therefore, we can neglect the influence of particle size on the TPR results. There are two reduction peaks in all the TPR profiles, which indicated that the reduction is composed of two steps, corresponding to the four and three coordinated Cu species respectively. As the reduction proceeds, Cl is removed from the catalyst by C_2H_4, Cu species changed from 4-coordinated to 3-coordinate, finally to 2-coordinate [37]. The deconvoluted TPR is shown in Fig. 3 and Table 2. The K-promoted catalyst shifted both the low and high-temperature peaks to a slightly higher temperature, indicating the K-promoted catalyst is more difficult to be reduced. The Mg promoter shifted significantly the two peaks to lower temperatures, indicating that the Mg promotes the $CuCl_2$ reduction. From the area contribution in Table 2, we can see the two peaks ascribed to the two-step reduction are

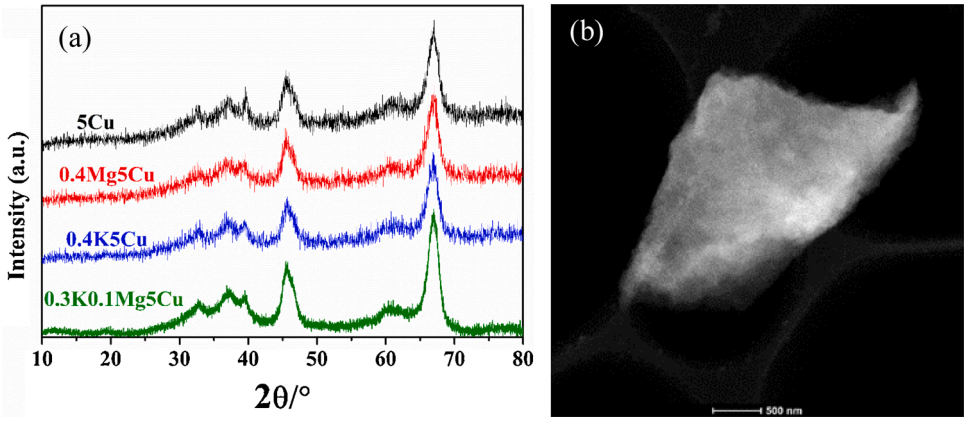

Fig. 1. (a) XRD profiles of the different catalysts; (b) TEM images of the 5Cu/Al_2O_3 catalyst.

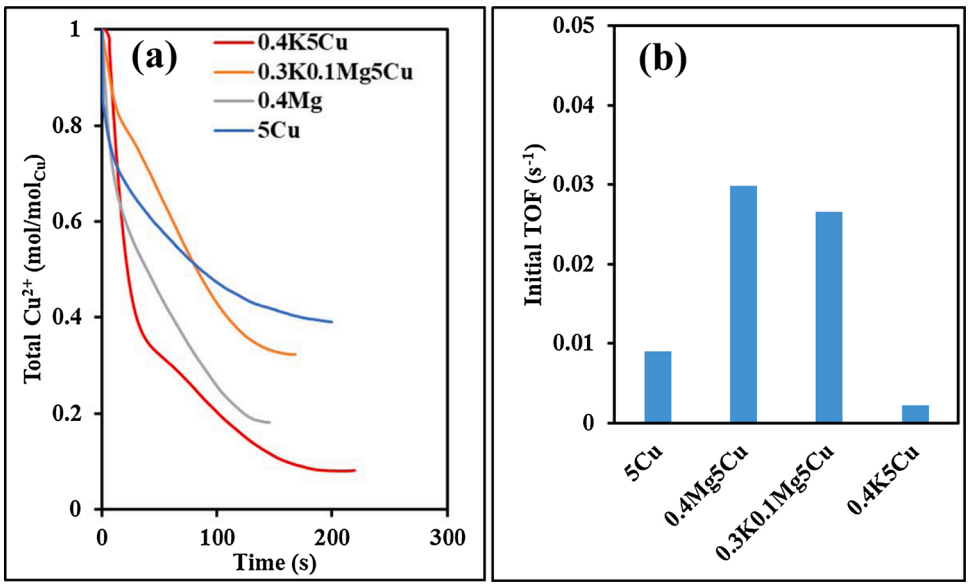

Fig. 2. (a) Cu^{2+} concentration with time on stream for the catalysts with and without promoters; (b) initial turnover frequency (TOF) of the reduction step for all the catalysts. Reaction conditions: W_{cat} = 0.3 g, T = 230 °C, P_{total} = 1 bar, $P_{C_2H_4}$ = 0.1 bar, F_{tot} = 180 ml/min.

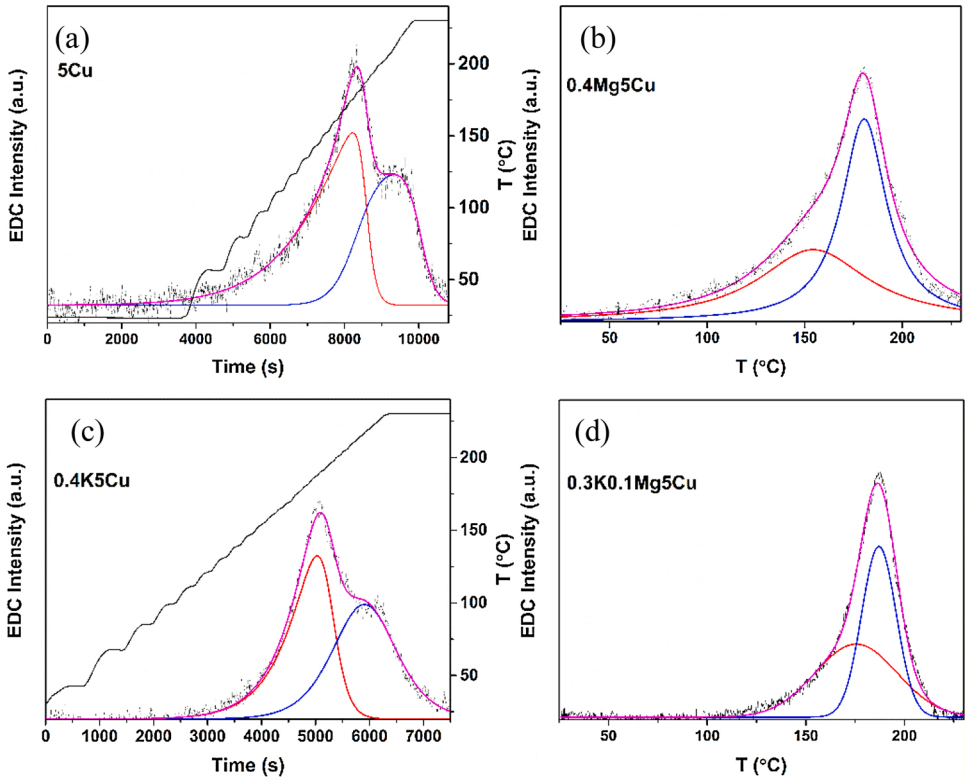

Fig. 3. TPR profiles for the (un)doped catalysts. Conditions: 0.3 g catalysts, F_{tot} = 120 ml/min, W_{cat} = 0.2 g, ramp rate: 2 °C/min, $P_{C_2H_4}$ = 0.3 bar.

Table 2
Summary of the TPR peaks position and area percentage.

Catalysts	T1/C	T2/C	A1/%	A2/%
5Cu	175.3	210.3	52.4	47.6
0.4K5Cu	187.7	216.4	51.1	48.9
0.4Mg5Cu	153.7	180.9	46.5	53.5
0.3K0.1Mg5Cu	175.0	188.1	50.4	49.6

quite close, indicating the Cu species changed from 4-coordinated to 3-coordinate, finally to 2-coordinate. We can also get the conclusion checking the ending of the TPR since the temperature is only increased to 230 °C, for the Mg-doped catalysts, the whole peaks can be obtained at the temperature of 230 °C. However, for 5Cu and 0.4K5Cu, only a half peak can be obtained at the temperature 230 °C, the TPR should be kept for a longer time to end the TPR. The temperature corresponding to the high-temperature peak follows the same order of the initial reduction rates of the catalysts: 0.4K5Cu<5Cu<0.3K0.1Mg5Cu<0.4Mg5Cu.

3.2.2. Kinetic analysis of CuCl oxidation

The kinetic performance of the oxidation step for the various catalysts is shown in Fig. 4. In the oxidation step, Cu^{+} was oxidized to Cu^{2+}, in the form of a copper oxychloride (Cu_2OCl_2). The total Cu^{2+} concentration increases with time on stream, as shown in Fig. 4a. By comparing with the reduction step of the neat 5Cu catalyst, we can find that the time required to complete the oxidation reaction is longer than that in reduction at the same partial pressure. It suggests that the oxidation reaction rate is much lower than the reduction rate for the neat 5Cu catalyst. The initial TOF of the oxidation for the various catalysts is also presented in Fig. 4b. The K promoted catalyst significantly increase the oxidation activity compared to the neat 5Cu catalyst, which was also studied in our previous report [23]. While, the only Mg-doped catalyst can also enhance the oxidation activity, although in a less magnitude compared to the K-doped catalyst. The co-doping catalyst, 0.3K0.1Mg5Cu behaves between 0.4Mg5Cu and 0.4K5Cu as we expected.

3.2.3. Use rate-diagram as a tool to predict the reaction rate and Cu oxidation state

The results in Fig. 2 and the literature studies [16,18,28,33] suggested that Cu^{2+} sites are the main active site, while the Cu^{+} sites are inactive. Therefore, the catalyst Cu^{2+} and Cu^{+} at the operational condition is a key parameter for the catalytic performance including activity and stability. Although the high activity of the catalyst is always desired, the stability of the catalyst is more important than the activity to avoid the Cu loss and migration thus the achieve a long lifetime. Therefore, the Cu^{2+} concentration is the most important parameter for catalyst design. We proposed previously a new tool of the kinetic diagram to predict the active Cu^{2+} based on the kinetics evolution of the reduction and oxidation steps in the transient experiments by studying the kinetics of neat Cu catalyst, and K or Ce promoted catalyst [16,22,23]. Both the reduction and oxidation rates can be correlated with the amount of Cu^{2+}. Since the third step of chlorination is a fast process and not kinetically relevant, thus it is not considered in the rate-diagram. Herein, we will use the rate-diagram to study the alkaline earth promoted and co-promoted catalysts. As shown in Fig. 5a-d, the reaction rates of both reduction and oxidation steps on the four catalysts plotted as a function of Cu^{2+} concentration. When the reaction reaches the steady-state, the reduction rate of reduction and oxidation should be identical, which is represented as the intersection of the two curves. The rate-diagram shows that the oxidation of Cu^{+} is low on the neat Cu catalyst leading to a high concentration of Cu^{+} at the steady-state. The K promoter reduced the reduction rates and increased the oxidation rate leading to a high Cu^{2+} concentration but a low steady-state reaction rate, while the Mg promoter increased both reduction and oxidation rates leading to a relatively high steady-state reaction rate but a relatively low Cu^{2+}. The predicted steady-state rate and Cu^{2+} concentration at the intersection points of the reduction and oxidation rate curves in the rate-diagram of the catalysts are shown in Fig. 5e. The results suggest that the Mg-doped catalyst can significantly increase the reduction rate, while the Cu^{2+} concentration remains the same with the neat 5Cu catalyst.

On the other hand, the K promoted catalyst, 0.4K5Cu increased the high Cu^{2+} concentration at the steady-state, about 0.83 mol/mol_{Cu}. But the activity was not significantly influenced compared to the neat 5Cu catalyst. Furthermore, by co-doping, the catalyst with Mg and K, which is named 0.3K0.1Mg5Cu, compromised the effect of K and Mg promoters and lead to both higher steady-state rate and Cu^{2+} concentration compared to Cu catalyst. However, it should be noted that the prediction of Cu^{2+} was carried out at a stochiometric feeding, but a relatively low partial pressure. The reduction and oxidation rates change with reaction conditions. It was reported that the first reaction order is with respect to ethylene and oxygen [38]. The reduction and oxidation rates change with reaction conditions. The apparent reaction order can be varied from 0 to 1, which depends on the adsorption strength on different materials. However, at the steady-state operation, both the reduction rate and oxidation rate changes with an identical factor of $P_{total}/(1+\sum K_i P_i)$, where P_{total} is the total pressure, P_i is the partial pressure of specie i and K_i is the equilibrium constant of the adsorption of specie i. Therefore, the Cu^{2+} predicted is also valid for the industrial conditions at the same temperature, regardless of the pressure.

3.3. Kinetic analysis of the steady-state experiments

The co-feeding or steady-state experiments for all the catalysts were performed at 230 °C and 1 bar, with the stoichiometric feed composition in Eq. 1, to validate the predicted steady-state rate and Cu^{2+} concentration. The evolution of the ethylene reaction rate for all the catalysts is shown in Fig. 6a. We can see the promoters have a positive effect on the catalytic performance, which is consistent with our previous reports. Herein, we can see the reaction rate in the experiment of the steady-state

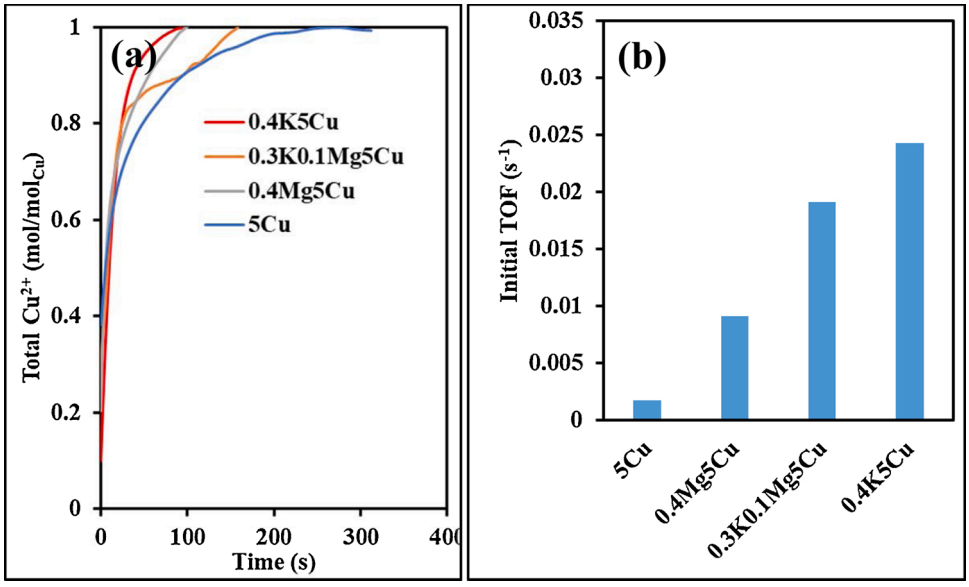

Fig. 4. (a) Cu^{2+} concentration with time on stream for the catalysts with and without promoters; (b) initial turnover frequency (TOF) of the oxidation step for all the catalysts. Reaction conditions: W_{cat} = 0.3 g, T = 230 °C, P_{total} = 1 bar, P_{O_2} = 0.1 bar, F_{tot} = 180 ml/min.

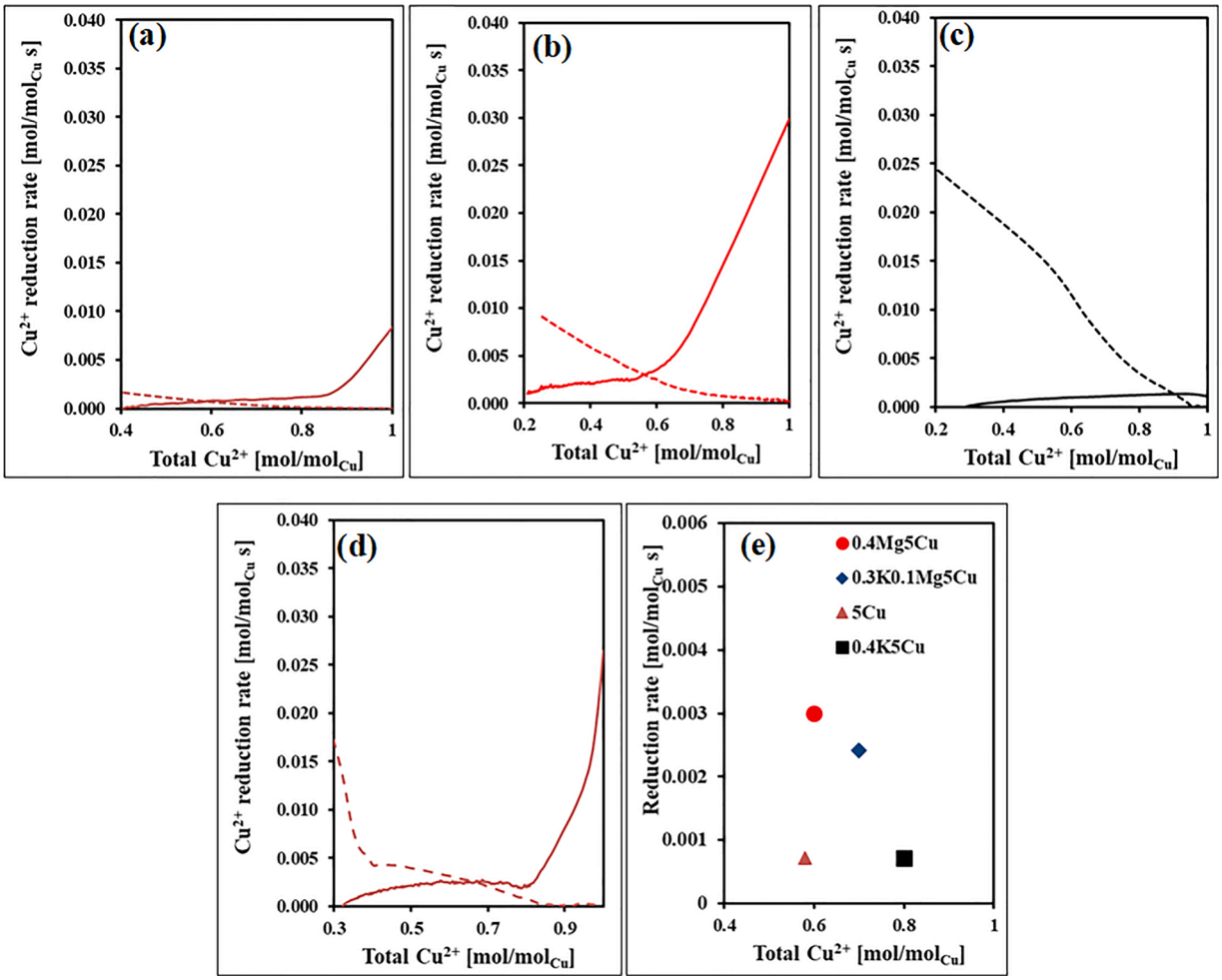

Fig. 5. Reaction rate-diagram of reduction (solid line) and oxidation (dashed line) steps on all the catalysts. (a) 5Cu; (b) 0.4Mg5Cu; (c) 0.4K5Cu; (d) 0.3K0.1Mg5Cu; (e) summary of the intersection points. Reaction conditions: W_{cat} = 0.3 g, T = 230 °C, P_{total} = 1 bar, $P_{C_2H_4}$ = 0.1 bar or P_{O_2} = 0.1 bar.

is quite close to that predicted by the rate-diagram, which further benchmarks the applicability of the rate-diagram. We have already known that the stability of ethylene oxychlorination is closely related to the Cu^{2+} concentration on the catalysts. So, we will study the effect of promoters on the Cu^{2+} concentration in the following.

As we previously reported, Cu^{2+} concentration profiles can be monitored by the operando UV–vis spectroscopy [16]. The Cu^{2+} concentration profiles at the top of the catalyst bed are shown in Fig. 6b. The tendency of the Cu^{2+} concentration is similar to the rate-diagram we discussed above. Which is, the K-doped catalyst has the highest Cu^{2+} retained on the catalyst than the other three. Which can be used to explain the most stable ethylene reaction rate in Fig. 6a. It is also confirmed by the intersection in the rate-diagram in Fig. 5e. While for the neat 5Cu catalyst, the Cu^{2+} concentration is the most less compared to the others. Based on our previous report and the above discussion, we know that the oxidation step is much slower than the reduction step, so the Cu cannot be regenerated to Cu^{2+} quickly, the result is Cu^{+} is the domain form on the catalyst. For the co-doping catalyst, 0.3K0.1Mg5Cu, it behaves between the mono-doping catalyst. It indicated that by co-doping the neat Cu catalyst with K and Mg, it could play a positive role in enhancing the reaction rate and Cu^{2+} concentration. For the promoted catalyst, the values between the predicted ones and the measured ones are quite close, indicating the rate diagram is a useful tool. While, for the neat Cu catalyst (without promoters), there is a deviation, caused by the copper loss. As we have discussed above that promoters are used to prevent the copper loss in the industry, also in our previous report [22]. In addition, no obvious peak for $CuCl_2$ was observed in the XRD patterns of the spent catalysts. For the clarity reason, the XRD patterns of the spent catalysts are not reported here. The results suggest that the promoted $CuCl_2$ still dispersed well on the Al_2O_3 surface after the reaction.

Fig. 6c shows the product selectivity of various promoted catalysts for the ethylene oxychlorination at 230 °C and 1 bar. For the neat Cu catalyst, the EDC selectivity is 92 %, about 8 % of the byproduct is ethyl chloride. While adding promoters into the catalysts can significantly prohibit the byproduct formation. K doped catalyst gave the highest EDC selectivity, there was no byproduct formed, followed by K, Mg co-doped catalyst 0.3K0.1Mg5Cu. However, the only Mg-doped catalyst gave a lower EDC selectivity compared to the co-doping catalyst, about 1% of C_2H_5Cl. Furthermore, the second analysis, which was roughly one hour after the first analysis was also performed and as shown in Fig. 6c. We can observe the byproduct formation increase along with time for the neat Cu catalyst. While, for Mg promoted catalyst, the selectivity of C_2H_5Cl was slightly increased (from 1.1 % to 1.3 %). Furthermore, the K, Mg co-doped catalyst also gave a slightly higher byproduct formation (from 0.6 % to 0.8 %). But the only K promoted catalyst was very stable, still, no byproduct was produced. The selectivity of the K and Mg co-promoted catalyst is also between the K and Mg mono-promoted catalysts. Comparing the neat Cu catalyst with the Mg-doped catalyst, the selectivity decreased from 8 % to 1 %, while the Cu^{+} is similar. It seems to indicate that the Cu^{+} is not the active site for the formation of ethyl chloride. It is most likely that the ethyl chloride is formed from the reaction of ethylene and HCl on the acidic sites on Al_2O_3, and K and Mg can titrate the acidic sites and suppress the reaction. The

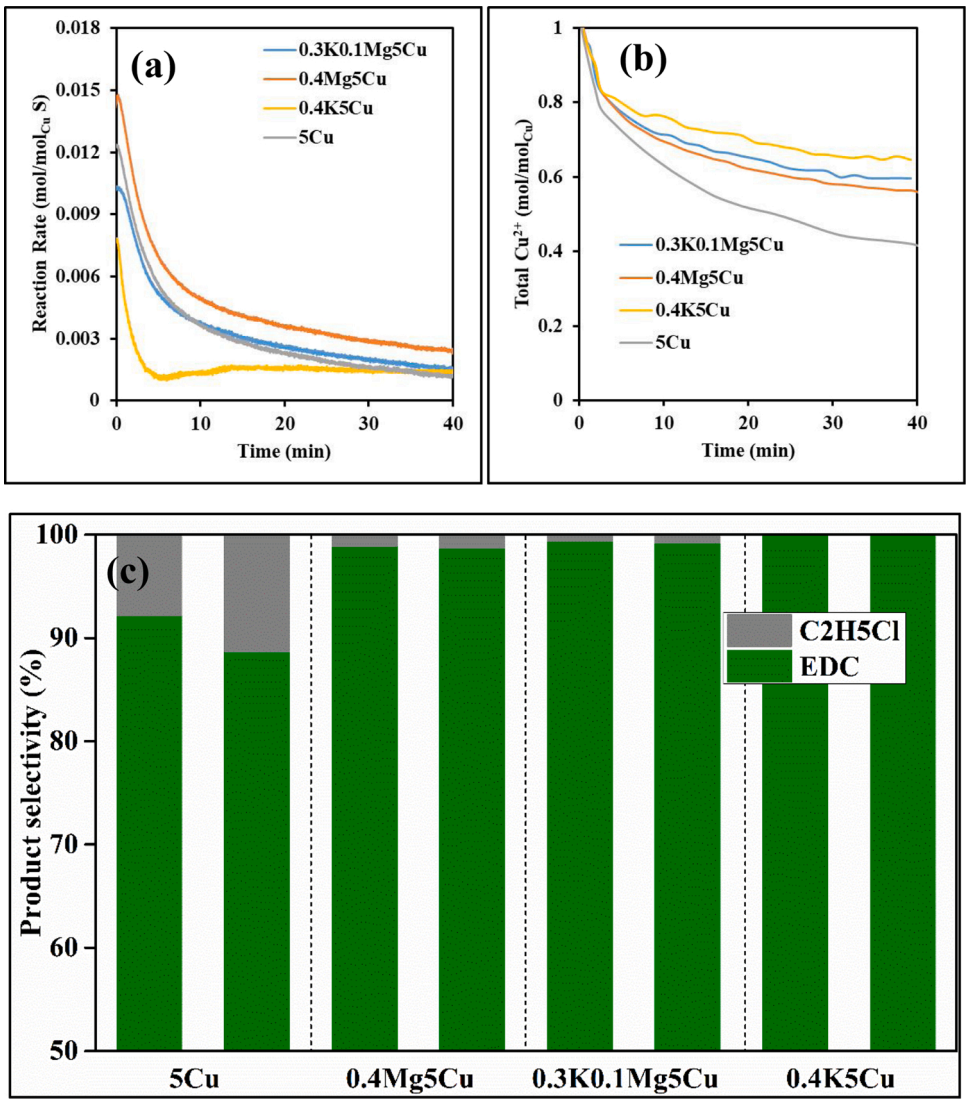

Fig. 6. Catalytic performance of the steady-state experiments for all the catalysts. (a) ethylene reaction rate with time on stream; (b) total Cu^{2+} profiles at the top of the catalyst bed with time on stream; (c) product selectivity during steady-state experiments, tested twice for each catalyst. Reaction conditions: $W_{cat} = 0.3$ g, T = 230 °C, $P_{total} = 1$ bar, $F_{tot} = 180$ ml/min, $P_{C_2H_4} = 0.08$ bar, $C_2H_4/O_2/HCl = 2:1:4$.

electronegativity of K (0.82) is lower than the one of Mg (1.31), indicate the higher basicity of K than the one of Mg. The stronger basic promoter K poisoned more the acidic sites and thus suppressed ethyl chloride formation more significantly compared to Mg. Also, no CO and CO_2 were detected most likely due to the low conversions at differential conditions, which are typically the product of the secondary reaction of EDC.

4. Conclusions

In summary, we have systematically studied the K and Mg co-promotion effect on $CuCl_2$-based catalysts for ethylene oxychlorination by applying a rate-diagram for the kinetic study. For the K doped catalyst, it enhanced the oxidation reaction rate a lot, while prohibiting the reduction step, and more Cu^{2+} was retained on the catalyst, which gives rise to high stability. While it is reverse for the Mg-doped catalyst, it increased the reduction rate more than the oxidation, which gives rise to less Cu^{2+} concentration and less stability compared to the K-doped catalyst. Furthermore, by co-doping K and Mg, both reduction and oxidation rete are enhanced compared to the neat Cu catalyst, which gives rise to both higher reaction rate and more Cu^{2+} concentration retained on the catalyst. Co-feeding or steady-state experiments were also performed to verify the reliability of the rate-diagram, the results show that the reaction rate at a steady state is quite close to that predicted by the rate-diagram. It was proved that rate-diagram is a reliable and easy method to study the kinetics of ethylene oxychlorination. The simple operando method is expected to be exploited for catalyst rational design and kinetic studies in the other redox catalytic reactions.

CRediT authorship contribution statement

Hongfei Ma: Conceptualization, Methodology, Validation, Formal analysis, Writing - original draft, Writing - review & editing. **Endre Fenes:** Validation, Writing - review & editing. **Yanying Qi:** Validation, Writing - review & editing. **Yalan Wang:** Validation, Writing - review & editing. **Kumar R. Rout:** Validation, Writing - review & editing, Supervision. **Terje Fuglerud:** Validation, Writing - review & editing. **De Chen:** Conceptualization, Methodology, Validation, Writing - review & editing, Supervision, Funding acquisition.

Declaration of Competing Interest

The authors declare that they have no known competing financial interests or personal relationships that could have appeared to influence the work reported in this paper.

Acknowledgments

The authors acknowledge the financial support from the industrial of Catalysis Science and Innovation (iCSI), a center for Research-based Innovation funded by the Research Council ofNorway under the grant No. of 237922.

References

[1] M.R. Flid, Catal. Ind. 1 (2010) 285–293.
[2] C.J. Davies, P.J. Miedziak, G.L. Brett, G.J. Hutchings, Chin. J. Catal. 37 (2016) 1600–1607.
[3] R. Lin, A.P. Amrute, J. Perez-Ramirez, Chem. Rev. 117 (2017) 4182–4247.
[4] X. Li, X. Pan, L. Yu, P. Ren, X. Wu, L. Sun, F. Jiao, X. Bao, Nat. Commun. 5 (2014) 3688.
[5] D. Shi, R. Hu, Q. Zhou, L. Yang, Chem. Eng. J. 288 (2016) 588–595.
[6] G. Malta, S.A. Kondrat, S.J. Freakley, C.J. Davies, L. Lu, S. Dawson, A. Thetford, E. K. Gibson, D.J. Morgan, W. Jones, P.P. Wells, P. Johnston, C.R.A. Catlow, C. J. Kiely, G.J. Hutchings, Science 355 (2017) 1399–1402.
[7] Q. Zhou, R. Hu, Y. Jia, H. Wang, Dalton Trans. 46 (2017) 10433–10439.
[8] Y. Sun, C. Li, Y. Guo, W. Zhan, Y. Guo, L. Wang, Y. Wang, G. Lu, Catal. Today 307 (2018) 286–292.
[9] M. Scharfe, P.A. Lira-Parada, V. Paunovic, M. Moser, A.P. Amrute, J. Perez-Ramirez, Angew. Chem. Int. Ed. 55 (2016) 3068–3072.
[10] C. Zipelli, J.C.J. Bart, G. Petrini, S. Galvagno, C. Cimino, Z. Anorg, Allg. Chem. 502 (1983) 199–208.
[11] C. Lamberti, C. Prestipino, F. Bonino, L. Capello, S. Bordiga, G. Spoto, A. Zecchina, S.D. Moreno, B. Cremaschi, M. Garilli, A. Marsella, D. Carmello, S. Vidotto, G. Leofanti, Angew. Chem. Int. Ed. 41 (2002) 2341–2344.
[12] D. Gianolio, N.B. Muddada, U. Olsbye, C. Lamberti, Nucl. Instrum. Methods Phys. Res. B. 284 (2012) 53–57.
[13] A. Montebelli, E. Tronconi, C. Orsenigo, N. Ballarini, Ind. Eng. Chem. Res. 54 (2015) 9513–9524.
[14] Z. Vajglová, N. Kumar, K. Eränen, M. Peurla, D.Y. Murzin, T. Salmi, J. Catal. 364 (2018) 334–344.
[15] Z. Vajglová, N. Kumar, K. Eränen, A. Tokarev, M. Peurla, J. Peltonen, D.Y. Murzin, T. Salmi, Appl. Catal. A 556 (2018) 41–51.
[16] K.R. Rout, E. Fenes, M.F. Baidoo, R. Abdollahi, T. Fuglerud, D. Chen, ACS Catal. 6 (2016) 7030–7039.
[17] E.M. Fortini, C.L. Garcia, D.E. Resasco, J. Catal. 99 (1986) 12–18.
[18] N.B. Muddada, U. Olsbye, L. Caccialupi, F. Cavani, G. Leofanti, D. Gianolio, S. Bordiga, C. Lamberti, Phys. Chem. Chem. Phys. 12 (2010) 5605–5618.
[19] N. Muddada, U. Olsbye, T. Fuglerud, S. Vidotto, A. Marsella, S. Bordiga, D. Gianolio, G. Leofanti, C. Lamberti, J. Catal. 284 (2011) 236–246.
[20] G. Leofanti, A. Marsella, B. Cremaschi, M. Garilli, A. Zecchina, G. Spoto, S. Bordiga, P. Fisicaro, C. Prestipino, F. Villain, C. Lamberti, J. Catal. 205 (2002) 375–381.
[21] K.S. Go, Y. Kim, S.R. Son, S.D. Kim, Chem. Eng. Sci. 65 (2010) 499–503.
[22] K.R. Rout, M.F. Baidoo, E. Fenes, J. Zhu, T. Fuglerud, D. Chen, J. Catal. 352 (2017) 218–228.
[23] M.F. Baidoo, E. Fenes, K.R. Rout, T. Fuglerud, D. Chen, Catal. Today 299 (2018) 164–171.
[24] G. Leofanti, M. Padovan, M. Garilli, D. Carmello, G.L. Marra, A. Zecchina, G. Spoto, S. Bordiga, C. Lamberti, J. Catal. 189 (2000) 105–116.
[25] G. Leofanti, M. Padovan, M. Garilli, D. Carmello, A. Zecchina, G. Spoto, S. Bordiga, G.T. Palomino, C. Lamberti, J. Catal. 189 (2000) 91–104.
[26] G. Leofanti, A. Marsella, B. Cremaschi, M. Garilli, A. Zecchina, G. Spoto, S. Bordiga, P. Fisicaro, G. Berlier, C. Prestipino, G. Casali, C. Lamberti, J. Catal. 202 (2001) 279–295.
[27] C. Lamberti, C. Prestipino, L. Capello, S. Bordiga, A. Zecchina, G. Spoto, S. Moreno, A. Marsella, B. Cremaschi, M. Garilli, Int. J. Mol. Sci. 2 (2001) 230–245.
[28] N.B. Muddada, U. Olsbye, G. Leofanti, D. Gianolio, F. Bonino, S. Bordiga, T. Fuglerud, S. Vidotto, A. Marsella, C. Lamberti, Dalton Trans. 39 (2010) 8437–8449.
[29] Y.-C. Xie, Y.-Q. Tang, Spontaneous monolayer dispersion of oxides and salts onto surfaces of supports: applications to heterogeneous catalysis, Adv. Catal. 37 (1990) 1–43.
[30] E. Finocchio, N. Rossi, G. Busca, M. Padovan, G. Leofanti, B. Cremaschi, A. Marsella, D. Carmello, J. Catal. 179 (1998) 606–618.
[31] C. Prestipino, S. Bordiga, C. Lamberti, S. Vidotto, M. Garilli, B. Cremaschi, A. Marsella, G. Leofanti, P. Fisicaro, G. Spoto, A. Zecchina, J. Phys. Chem. B 107 (2003) 5022–5030.
[32] M.J. Louwerse, G. Rothenberg, ACS Catal. 3 (2013) 1545–1554.
[33] N.B. Muddada, T. Fuglerud, C. Lamberti, U. Olsbye, Top. Catal. 57 (2013) 741–756.
[34] R.A. Schoonheydt, Chem. Soc. Rev. 39 (2010) 5051–5066.
[35] G.C. Bond, S.N. Namijo, J.S. Wakeman, J. Mol. Catal. 64 (1991) 305–319.
[36] A. Rouco, Appl. Catal. A 117 (1994) 139–149.
[37] Y. Qi, E. Fenes, H. Ma, Y. Wang, K.R. Rout, M. Piccinini, T. Fuglerud, D. Chen, J. Phys. Chem. C. 124 (2020) 10430–10440.
[38] Y.A. Treger, V.N. Rozanov, M.R. Flid, L.M. Kartashov, Russ. Chem. Rev. 57 (1988) 326.